The Influence of Aluminum on Indium and Tin Behaviour During Secondary Copper Smelting

Katri Avarmaa and Pekka Taskinen

Abstract Aluminum and copper are large volume metals in electronic appliances, while tin and indium exist as common minor elements. All of these non-ferrous metals are aimed to be separated and recycled from the end-of-life electronics into non-ferrous scrap fraction(s), and further through pyrometallurgical and/or hydrometallurgical processes to pure metals. Depending on the mechanical pre-treatment processes, aluminum and copper liberation from each other varies. This study focuses on the influence of alumina on indium and tin distributions between copper alloy and iron silicate slags with 0, 9 and ~16 wt% of Al_2O_3. The experiments were executed with an equilibration-quenching-EPMA technique in an oxygen pressure range of 10^{-10}–10^{-5} atm at 1300 °C. The metal-slag distribution coefficient of indium remains constant as a function of alumina in slag, while that of tin increases. Therefore, aluminum in feed or alumina addition to the slag improves the recovery of tin into copper. Nevertheless, oxygen pressure has clearly more significant influence on the behavior of both the metals in the smelting conditions.

Keywords Recovering · Technical metals · Sustainability

Introduction

Secondary copper plants employ different type of waste sources as raw materials including ashes, slags, dusts, drosses, anode slimes, metallic scraps and waste electric and electronic equipment (WEEE) [1, 2]. Factories may use all of these sources, are only focused on certain type of waste stream(s) or possibly employ them along with primary concentrate. As a result, every plant is unique and the smelting will include

K. Avarmaa (✉) · P. Taskinen
School of Chemical Engineering, Department of Chemical and Metallurgical Engineering, Aalto University, PO Box 16100, 00076 Aalto, Finland
e-mail: katri.avarmaa@aalto.fi

B. Davis et al. (eds.), *Extraction 2018*, The Minerals, Metals & Materials Series,
https://doi.org/10.1007/978-3-319-95022-8_85

various elements—impurities and valuable, rare ones—in various quantities. This study focuses on utilizing an end-of-life copper (of WEEE) including indium and tin traces with different amounts of unliberated aluminum.

WEEE composition varies greatly through different e-products (what, when and where product is produced and disposed), which makes it difficult to generalize the composition of the entire waste stream. Some general estimations [3–5] propose that WEEE comprises approximately 60% metals, 20% plastics and rest glass/screens (>10%), cables, PCBs (printed circuit boards), pollutants etc. (which actually also include metals). During the past ten-twenty years, the demand for technical rare metals, such as indium [6], has increased drastically in order to fulfill specific property requirements of the modern electronics. Multiple rare and valuable elements even exist at higher concentrations in WEEE than in their respective ores [7] making WEEE highly potential and important secondary resource for these metals. As a result, the secondary production of base and minor elements increases continuously and recovering of different minor elements is becoming economically and environmentally feasible over time.

The actual recovery process after disposing and transporting starts with the mechanical shredding and separation processes. The most common, recycled non-ferrous metals are aluminum and copper. Depending on the recycling facility, non-ferrous metals are separated into one scrap fraction, such as Zorba [8], or multiple fractions. Especially aluminum is often aimed at liberating from the rest of the non-ferrous metals. Nevertheless, the liberation of aluminum from copper is not complete and some portion will be sorted into wrong fraction(s) [9, 10]. Moreover, PBCs that are directly introduced into the smelting furnace include varying concentrations of aluminum [9, 11]. The fractions where metals end up after mechanical shredding and separation are dependent on many factors, such as the e-waste composition, target fraction compositions, mechanical recycling processes/techniques and their liberation efficiencies.

When aluminum in copper scrap or e-scrap (PCBs) is fed into the smelting furnace, it oxidizes into alumina and becomes part of the slag phase. Thus, it has clear influence on the slag composition and properties, and further on the whole process and on the minor element behavior. Typical primary and secondary copper smelting slags are iron-silicate based with some fractions of CaO, Al_2O_3, MgO and other oxides and impurities [2, 12]. Figure 1 presents a phase diagram of FeO–SiO_2–Fe_2O_3–10 wt% Al_2O_3 slag and Fig. 2 that of pure iron-silicate, with oxygen activity contours superimposed. The diagrams were calculated with MTDATA employing MTOX database vers 8.1 [13].

The liquid phase boundaries and liquid phase position of FeO–SiO_2–Fe_2O_3–$10Al_2O_3$ slag are clearly different when compared to the traditional ternary FeO–SiO_2–Fe_2O_3 phase diagram. Alumina addition increases remarkably silica solubility in the oxide liquid phase, and moves the liquid region towards the silica corner. In this study, we follow the liquid-tridymite phase boundaries in Figs. 1 and 2, and a

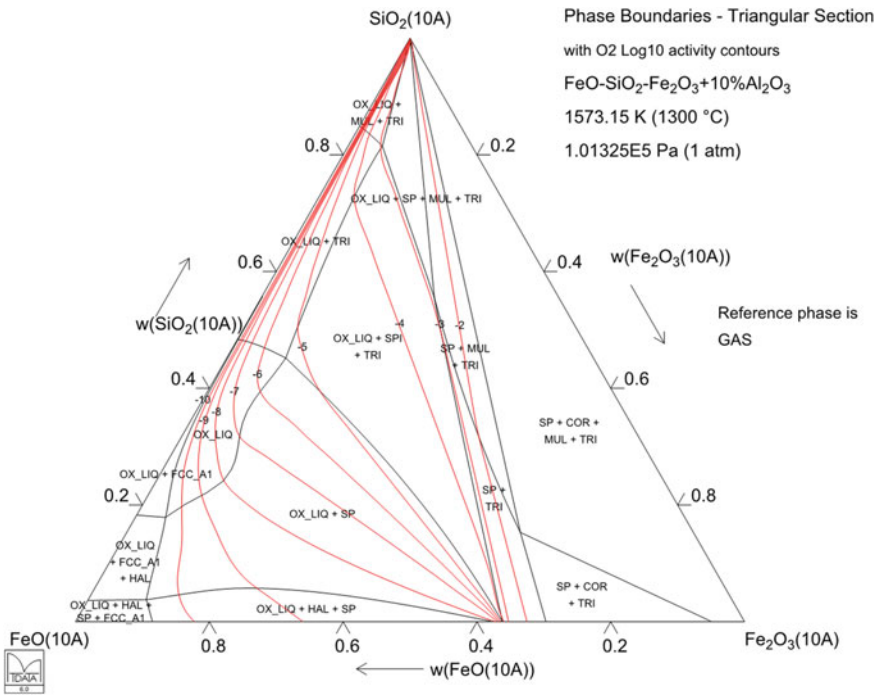

Fig. 1 $FeO–SiO_2–Fe_2O_3–10Al_2O_3$ phase diagram with oxygen isobars, MTDATA (w is weight fraction)

liquid-spinel(-mullite) phase boundary at indirect alumina saturation [14]. The phase diagrams in Figs. 1 and 2 do not take copper into account, and especially at high oxygen partial pressures, copper solubility in slag will have a great influence on the liquid phase region [14]. Thus, the presented phase diagrams are not directly comparable to our experimental conditions and results at 10^{-5} atm.

Alumina has amphoteric nature in silicate melts [15]. Thus, how alumina is coordinated in the system is dependent on the base slag and the ratio of basic/acidic oxides in the system. The amphoteric behavior of alumina in melts, slags and glasses has been investigated quite broadly by measuring physical properties such as density, viscosity, surface tension, thermal and electrical conductivity [15–18]. As alumina influences the chemical and physical properties of the slags, naturally it has an influence on the minor element behavior, too. This study explores the dependency of indium and tin behavior on alumina content in iron silicate slag. The experiments were executed in simulated secondary copper smelting conditions from reducing to oxidizing conditions.

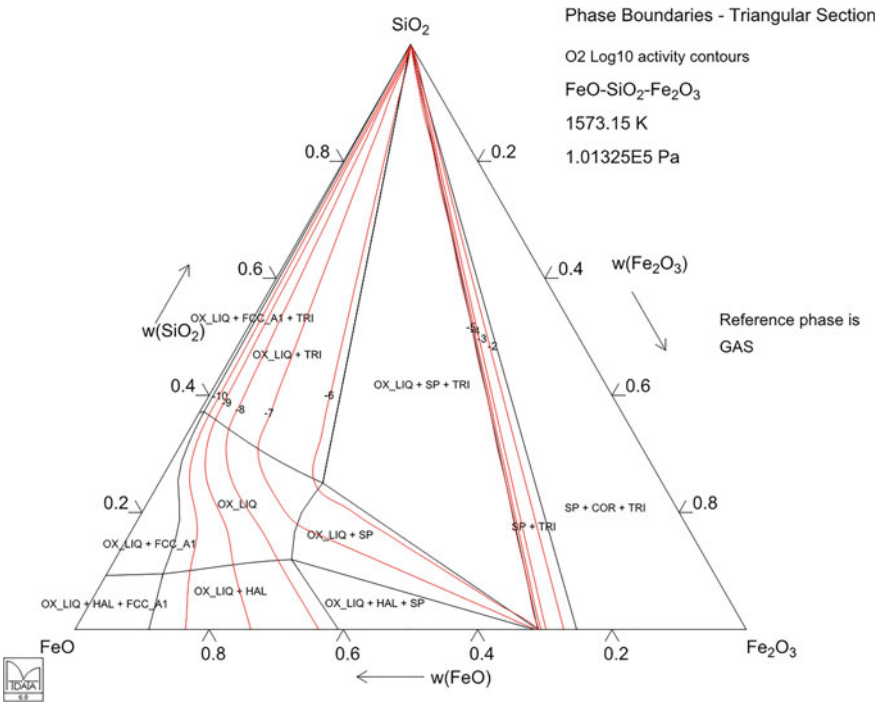

Fig. 2 $FeO–SiO_2–Fe_2O_3$ phase diagram with oxygen isobars

Experimental Procedure

Experimental technique was a modern equilibration-quenching method, which is typical for the phase equilibria [19, 20] and minor element investigations [21]. The equilibration experiments were conducted in a vertical tube furnace, Nabertherm RHTV 120-150/18 with $MoSi_2$ heating elements and an alumina reaction tube. Figure 3 presents a photograph of the employed furnace highlighting some of its main parts.

The gas atmosphere was controlled with thermal mass flow controllers (Aalborg, 052-01-SA) of CO and CO_2 gases. With a certain CO_2/CO flow ratio, the experimental atmosphere responded to specific pO_2, between 10^{-10} and 10^{-5} atm at the experimental temperature. The sufficient equilibration time for experiments were defined with a time series from 1 h to 32 h, changing starting compositions and pre-heating a sample at 1350 °C for 30 min prior to the actual equilibration period. According to the pre-experiment data, the equilibration time for each sample was set 16 h to ensure the equilibrium in each condition. The samples were quenched after experiments in brine or ice water mixture. More details about the technique, assembly and electron micro probe analyses can be found in our previous publications [14, 22].

Fig. 3 Equilibration furnace

The copper master alloy including initially approximately 1 wt% of indium and 1 wt% of tin was prepared in sealed silica ampoule at 1200 °C [14]. The slags were powder mixtures comprising Fe_2O_3, SiO_2 and Al_2O_3. All the reagent chemicals were from Alfa Aesar or Sigma-Aldrich with a purity of 99.9% or higher. Two type of crucibles were used, silica (Heraeus HSQ® 300, Electrically fused quartz, >99.998%) and alumina (Degussit AL23, >99.5%) ones. For the experiments executed in alumina crucibles, the initial slag powder mixture was constant at Fe/SiO_2 ratio of 1.3 (w/w) with 20 wt% of Al_2O_3. For the silica-saturated iron silicate slags, the initial composition was set to 30 wt% SiO_2–70Fe_2O_3 and for the duplicate series to 25 wt% SiO_2–75Fe_2O_3. Whereas, for the iron silicate slags including 10 wt% of Al_2O_3 at silica saturation, the initial slag mixture varied for different oxygen pressures in order to keep the alumina concentration constant at every experimental condition. These compositions for each oxygen pressure were defined with a preliminary test series.

Equivalent masses of copper alloy and slag mixture, 0.08–0.25 g each, were pressed to pellets in the experiments employing silica crucibles or put as such (alloy pieces and slag powder) in the alumina crucibles. After equilibration and quenching the sample, it was prepared employing wet metallographic techniques for SEM-EDS and EPMA analyses. Liquid phases and the primary solid phases were analysed with EPMA, providing the following results.

Results and Discussion

Elemental results for copper and slag phases are represented in Table 1. Tridymite was analyzed only from selected samples covering the whole oxygen partial pressure range. These show that it composed of SiO_2 with traces of copper and iron, with less than 1 wt% each. Indium and tin were below the detection limits (<110 ppm) in every condition. Spinel results can be seen in our previous paper [14].

Equilibria Systems

The Equilibrium systems included two liquid phases—copper and slag—either at tridymite (SiO_2) saturation or spinel saturation. Typical micrographs for both cases are presented in Fig. 4. Most of the samples had entirely homogeneous slag structures, and only at the highest pO_2 slags had some copper segregations.

As shown previously, we follow two different liquidus lines in this study. The iron-to-silica ratio as a function of alumina in slag is presented in Fig. 4. With pure iron silicate slags at silica saturation and with spinel saturated slags, the iron-to-silica ratios are in the same range, around 1.2. When alumina is added in silica saturated slag the Fe/SiO_2 ratio drops to half or more, and the drop increases as a function of increasing oxygen partial pressure.

These silica-saturated points in Fig. 4 can be compared to the previously presented phase diagrams at pO_2 conditions $\leq 10^{-7}$ atm (Figs. 1 and 2). According to the phase diagrams, the Fe/SiO_2 ratios of FeO_x–SiO_2 and FeO_x–SiO_2–$10Al_2O_3$ are around 0.85 and 1.6, respectively. Our experimental results (Fig. 5) show lower Fe/SiO_2 ratios. Moreover, according to the phase diagram in Fig. 1, the ratio decreases with decreasing pO_2 contrary to our experimental results.

Copper solubility in each slag is presented in Fig. 6. Alumina content in slag or the saturation phase did not have a clear influence on the copper solubility. All the obtained points fit well with each other providing similar trends. The slopes were for silica-saturated slags 0.26–0.30 and for spinel saturated 0.30. These indicate strongly to $CuO_{0.5}$ form (Cu^{1+}).

Figures 7 and 8 present the distribution coefficients of indium and tin as a function of Al_2O_3 in slag under three oxygen partial pressures. Distribution coefficient is defined as weight ratio of element-of-interest (Me) between two phases, in this case copper and slag as:

$$L^{Cu/s}[Me] = wt\%[Me]_{copper}/wt\%(Me)_{slag}.$$

At reducing conditions, the distribution coefficients of indium and tin are around 10. Therefore, they are distributed approximately at 90% in the copper phase, over the slag phase. Whereas in the most oxidizing conditions, tin and indium distribution coefficients are around 0.1 and 0.04, respectively. Thus, approximately

Table 1 Normalized averages and standard deviations for elements in slag and copper phases

			Slag phase							Copper phase			
	No.	$lgpO_2$	O	Si	Al	Cu	Fe	In	Sn	Cu	Fe	In	Sn
FeO_x–SiO_2	1	−9	35.06 ± 0.21	17.32 ±0.10		1.44 ± 0.02	45.36 ± 0.18	0.01	0.04	98.88 ± 0.13	0.22 ± 0.01	0.12 ± 0.01	0.25 ± 0.02
	2	−7	34.38 ± 0.70	15.72 ± 0.22		5.08 ± 0.17	43.82 ± 0.88	0.13 ± 0.01	0.03	99.09 ± 0.10	0.03	0.08	0.02
	3	−7	35.61 ± 0.55	15.98 ± 0.50		4.99 ± 0.09	42.47 ± 0.27	0.10 ± 0.01	0.03	99.29 ± 0.08	0.02	0.07	0.02
	4	−5	30.82 ± 0.55	13.15 ± 0.36		22.58 ± 1.08	32.39 ± 0.25	0.46 ± 0.01	0.06	98.67 ± 0.15	0.003 (<DL)	0.01	0.004 (<DL)
	5	−5	31.25 ± 0.35	12.67 ± 0.16		23.13 ± 0.40	31.80 ± 0.19	0.49 ± 0.01	0.05	98.69 ± 0.19	0.008 (<DL)	0.02	0.003 (<DL)
FeO_x–SiO_2–$10Al_2O_3$	6	−9	39.60 ± 0.11	20.73 ± 0.27	4.21 ± 0.07	1.53 ± 0.05	33.28 ± 0.19	0.03	0.04	98.33 ± 0.13	0.17 ± 0.01	0.34 ± 0.04	0.51 ± 0.06
	7	−9	38.80 ± 0.16	21.44 ± 0.07	4.26 ± 0.28	1.55 ± 0.07	33.28 ± 0.15	0.04	0.04	98.30 ± 0.11	0.17 ± 0.01	0.34 ± 0.01	0.49 ± 0.03
	8	−7	38.84 ± 0.30	20.95 ± 0.09	4.87 ± 0.49	5.85 ± 0.14	28.61 ± 0.15	0.21 ± 0.01	0.02	99.06 ± 0.12	0.02	0.16 ± 0.02	0.04
	9	−7	39.36 ± 0.09	21.16 ± 0.07	4.50 ± 0.11	5.77 ± 0.06	28.26 ± 0.13	0.27 ± 0.01	0.05	99.12 ± 0.13	0.02	0.20 ± 0.02	0.05
	10	−5	38.47 ± 0.41	22.28 ± 0.23	4.94 ± 0.20	17.26 ± 0.62	16.13 ± 0.12	0.43 ± 0.01	0.03	99.13 ± 0.07	0.008 (<DL)	0.03	0.006 (<DL)
	11	−5	38.33 ± 0.50	22.71 ± 0.30	4.82 ± 0.21	17.23 ± 0.73	15.99 ± 0.19	0.42 ± 0.00	0.03	99.13 ± 0.07	0.005 (<DL)	0.02	0.005 (<DL)
FeO_x–SiO_2–$16Al_2O_3$	12	−9	36.19 ± 0.13	14.20 ± 0.09	8.64 ± 0.07	1.32 ± 0.01	38.93 ± 0.12	0.06	0.03	97.26 ± 0.10	0.22 ± 0.01	0.80 ± 0.05	0.79 ± 0.05
	13	−9	35.46 ± 0.19	14.75 ± 0.10	9.32 ± 0.20	1.41 ± 0.01	38.09 ± 0.29	0.07	0.03	97.09 ± 0.17	0.21 ± 0.01	0.78 ± 0.09	0.76 ± 0.08
	14	−7	35.95 ± 0.40	14.43 ± 0.08	8.47 ± 0.08	5.28 ± 0.09	34.21 ± 0.22	0.47 ± 0.01	0.19 ± 0.01	98.32 ± 0.08	0.02	0.30 ± 0.03	0.41 ± 0.03
	15	−7	35.74 ± 0.28	14.49 ± 0.13	9.45 ± 0.16	5.41 ± 0.02	33.62 ± 0.12	0.51 ± 0.01	0.19 ± 0.01	98.35 ± 0.10	0.02	0.35 ± 0.02	0.41 ± 0.03
	16	−5	33.97 ± 0.31	9.59 ± 0.08	7.45 ± 0.06	21.02 ± 0.45	26.13 ± 0.22	0.66 ± 0.01	0.42 ± 0.01	98.65 ± 0.08	0.01	0.02	0.05
	17	−5	32.71 ± 0.14	9.78 ± 0.08	7.97 ± 0.06	22.33 ± 0.32	25.53 ± 0.21	0.64 ± 0.01	0.40 ± 0.01	98.04 ± 0.30	0.01	0.02	0.05

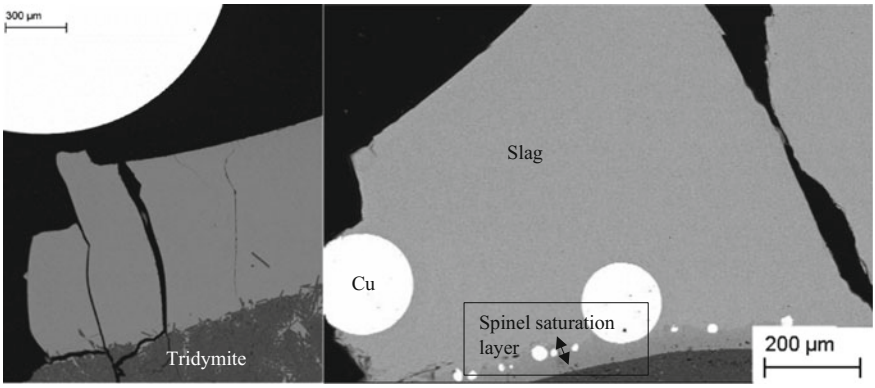

Fig. 4 BSE micrographs in typical copper/slag/tridymite (left side) and copper/slag/spinel/alumina (right side) samples at 10^{-7} atm and 1300 °C

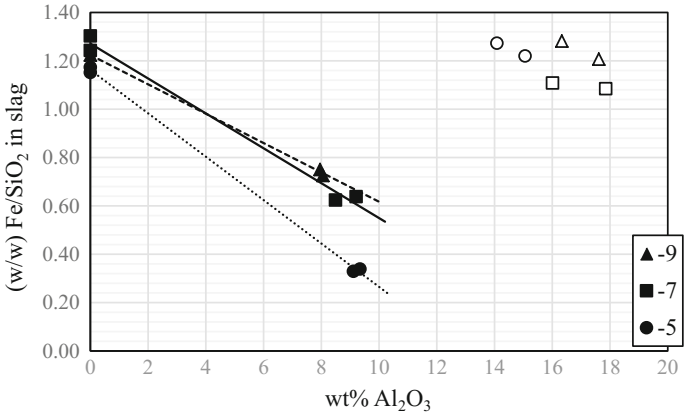

Fig. 5 Fe/SiO_2 ratio as a function of alumina concentration in slag for three logarithmic oxygen partial pressures. Open symbols indicate the spinel saturated slags, whereas closed refer to the silica saturated slags

Fig. 6 Copper solubility as a function of oxygen partial pressure in three different slags at 1300 °C

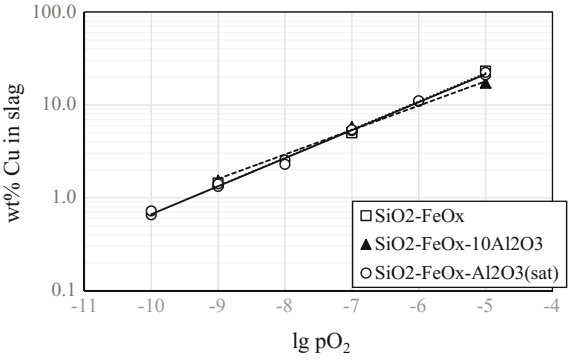

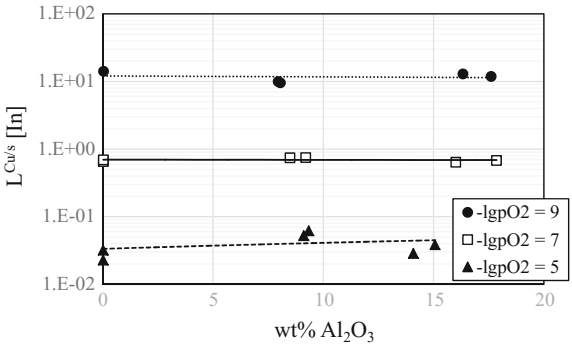

Fig. 7 Metal-slag distribution coefficient of indium as a function of alumina in slag at 1300 °C and 10^{-9}, 10^{-7} or 10^{-5} atm

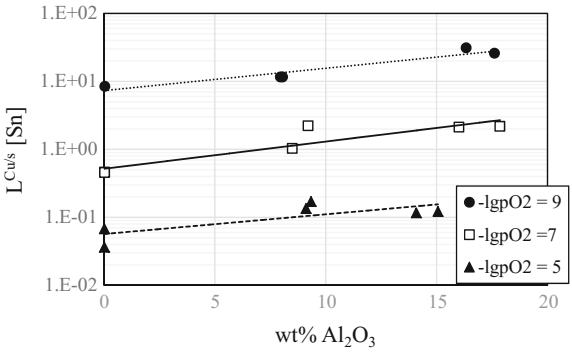

Fig. 8 Metal-slag distribution coefficient of tin as a function of alumina in slag at 1300 °C and 10^{-9}, 10^{-7} or 10^{-5} atm

90–95% of In and Sn are lost in slag when compared to their solubilities into the copper phase. Alumina addition or the saturation phase did not have influence on the behavior of indium according to our results. On tin instead, alumina seems to have a positive influence if considering recoveries into the copper phase.

Overall, tin and indium can be deported into the liquid phases—copper and slag—or the solid tridymite/spinel or the gas phase. Tridymite did not dissolve tin or indium according to our EPMA results. Spinel, instead, dissolved increasing concentrations of indium and tin as a function of increasing oxygen partial pressure [d], even up to 0.4 wt% In ($L^{sp/s}$[In] = 0.4) at $pO_2 = 10^{-5}$ atm. At spinel saturation part of the tin vaporized from the samples at $pO_2 = 10^{-5}$ atm [14], and at silica saturation, almost all tin was vaporized at $pO_2 = 10^{-7}$–10^{-5} atm. Thus, tin recovery after oxidizing process step should be performed mainly from the process flue dusts.

According to our results, excess aluminum in copper scrap smelting will not have negative influence on the recovery possibilities of these elements, and tin recovery in copper over slag is even improved. Anyhow, it will have an influence on the produced slag composition, slag volume and possible solid phase formation.

Therefore, process changes, in order to improve metal yields, need to be done with a comprehensive overview of the process, environment, economy and the other essential aspects.

Conclusions

This study experimentally examined the influence of alumina concentration (0, 9 and 16 wt%) in slag into the distribution coefficients of indium and tin between metallic copper and Al_2O_3–FeO_x–SiO_2 slags. Experiments were executed in typical black copper smelting conditions at 1300 °C and $pO_2 = 10^{-10}$–10^{-5} atm, employing the equilibrium-quenching technique with EPMA. Alumina or the saturation phase (silica or spinel) did not have influence on the copper solubility in slags or on the indium distribution behavior. Whereas tin behavior was dependent on the alumina concentration in slag, and alumina improved its recovery possibilities to copper. Nevertheless, at 10^{-5}–10^{-7} atm tin was mainly vaporized from the samples.

Acknowledgements This work was supported by Tekes (currently Business Finland) and CLEEN Oy (Clic Innovation Oy) through ARVI project. We also want to acknowledge Lassi Pakkanen for executing the EPMA analyses, Simon Yliaho on experimental help and Lassi Klemettinen on the preliminary SEM-EDS analysis.

References

1. Lehner T (1998) Integrated recycling of non-ferrous metals at Boliden Ltd. Rönnskar smelter. In: Proceedings of the 1998 IEEE international symposium on electronics and the environment. IEEE, pp 42–47
2. Schlesinger ME, King MJ, Sole KC, Davenport WG (2011) Extractive metallurgy of copper. Elsevier, UK
3. Khaliq A, Rhamdhani MA, Brooks G, Masood S (2014) Metal extraction processes for electronic waste and existing industrial routes: a review and Australian perspective. Resources 3(1):152–179
4. Widmer R, Oswald-Krapf H, Sinha-Khetriwal D, Schnellmann M, Böni H (2005) Global perspectives on e-waste. Environ Impact Assess Rev 25(5):436–458
5. Işıldar A, Rene ER, van Hullebusch ED, Lens PN (2017) Electronic waste as a secondary source of critical metals: management and recovery technologies. Resour Conserv Recycl. https://doi.org/10.1016/j.resconrec.2017.07.031
6. Zhang S, Ding Y, Liu B, Chang CC (2017) Supply and demand of some critical metals and present status of their recycling in WEEE. Waste Manag 65:113–127
7. Takahashi KI, Tsuda M, Nakamura J, Otabe K, Tsuruoka M, Matsuno Y, Adachi Y (2009) Elementary analysis of mobile phones for optimizing end-of-life scenarios. In: IEEE international symposium on sustainable systems and technology. IEEE
8. Kelly S, Apelian D (2016) Scrap characterization to optimize the recycling process. REWAS 2016. Springer, Cham, pp 227–229

9. Veit HM, Bernardes AM, Ferreira JZ et al (2006) Recovery of copper from printed circuit boards scraps by mechanical processing and electrometallurgy. J Hazard Mater 137(3): 1704–1709
10. Andersen MS, Thomsen M (2012) Greening of electronics. Environmental project No. 1416. The danish environmental protection agency, Denmark. https://www.researchgate.net/profile/Massimo_Pizzol/publication/251880557_Greening_of_Electronics/links/0c96053760f439d385000000/Greening-of-Electronics.pdf. Accessed 12 February 2018
11. Oguchi M, Murakami S, Sakanakura H, Kida A, Kameya T (2011) A preliminary categorization of end-of-life electrical and electronic equipment as secondary metal resources. Waste Manag 31(9–10):2150–2160
12. Gorai B, Jana RK (2003) Characteristics and utilisation of copper slag—a review. Resour Conserv Recycl 39(4):299–313
13. Gisby J, Taskinen P, Pihlasalo J, Li Z, Tyrer M, Pearce J et al (2017) MTDATA and the prediction of phase equilibria in oxide systems: 30 years of industrial collaboration. Metall Mater Trans B 48(1):91–98
14. Avarmaa K, Yliaho S, Taskinen P (2018) Recoveries of rare elements Ga, Ge, In and Sn from waste electric and electronic equipment through secondary copper smelting. Waste Manag 71:400–410
15. Park JH, Min DJ, Song HS (2004) Amphoteric behavior of alumina in viscous flow and structure of CaO–SiO_2 (–MgO)–Al_2O_3 slags. Metall Mater Trans B 35(2):269–275
16. Mostaghel S, Matsushita T, Samuelsson C, Björkman B, Seetharaman S (2013) Influence of alumina on physical properties of an industrial zinc-copper smelting slag Part 1—viscosity. Miner Process Extractive Metall 122(1):42–48
17. Mostaghel S, Matsushita T, Samuelsson C, Björkman B, Seetharaman S (2013) Influence of alumina on physical properties of an industrial zinc–copper smelting slag Part 2—apparent density, surface tension and effective thermal diffusivity. Miner Process Extr Metall 122(1): 49–55
18. Doweidar H (1998) Density–structure correlations in Na_2O–Al_2O_3–SiO_2 glasses. J Non-Cryst Solids 240(1–3):55–65
19. Hamuyuni J, Taskinen P (2016) Experimental phase equilibria of the system Cu–O–CaO–Al_2O_3 in air. J Eur Ceram Soc 36(3):847–855
20. Hidayat T, Henao HM, Hayes PC, Jak E (2012) Phase equilibria studies of Cu–O–Si systems in equilibrium with air and metallic copper and Cu–Me–O–Si systems (Me = Ca, Mg, Al, and Fe) in equilibrium with metallic copper. Metall Mater Trans B 43(6):1290–1299
21. Avarmaa K, O'Brien H, Johto H, Taskinen P (2015) Equilibrium distribution of precious metals between slag and copper matte at 1250–1350C. J Sustain Metall 1(3):216–228
22. Klemettinen L, Avarmaa K, Taskinen P (2017) Slag Chemistry of High-Alumina Iron Silicate Slags at 1300 °C in WEEE Smelting. J Sustain Metall 3(4):772–781